Development Of A Stitched/RFI Composite Transport Wing

Yury Kropp
McDonnell Douglas Aerospace-Transport Division
Long Beach, CA

Abstract

Development of a composite wing primary structure for commercial transport aircraft is being undertaken at McDonnell Douglas under NASA contract. The focus of the program is to design and manufacture a low cost composite wing which can effectively compete with conventional metal wing structures in terms of cost, weight and ability to withstand damage. These goals are being accomplished by utilizing the stitched/RFI manufacturing process during which the dry fiber preforms consisting of several stacks of warp-knit material are stitched together, impregnated with resin and cured. The stitched/RFI wing skin panels have exceptional damage tolerance and fatigue characteristics, are easily repairable, and can carry higher gross stress than their metal counterparts. This paper gives an overview of the program, describes the key features of the composite wing design and addresses major issues on analysis and manufacturing.

Introduction

The development of transport aircraft composite primary wing structure has been under study at McDonnell Douglas since 1975. The original design concept was based on the prepreg tape material designed to the ultimate micro-strain level of 4500 for damage tolerance. However, it become evident that this conventional prepreg approach was not likely to lead to a cost effective application of composite materials to primary wing structure. The stitched dry preform/resin film infusion process was selected as having the best potential for achieving target weight and cost goals.

In the S/RFI process the dry fiber preforms arranged in stacks are stitched through the thickness with a multi-needle machine, are impregnated with resin and cured in an autoclave (Figure. 1). Besides improving damage resistance and tolerance of the cured part, stitching also provides the compaction necessary for the assembly of inner mold line (IML) tooling, enhances the flow of resin in the infusion process, and virtually eliminates stiffener separation and other secondary failure of an interlaminar nature.

A primary objective of the "Innovative Composite Aircraft Primary Structure" (ICAPS) program is to develop the technology to allow the incorporation of an all-composite wing on a commercial transport aircraft. The baseline aircraft selected for this study is a new McDonnell Douglas MD-XX advanced technology twin-engined aircraft (Figure 2). The aircraft configuration is designed to carry 192 passengers in a two-class arrangement. Composites will make up 39% of the airframe weight (Figure 3), a significant increase from the MD-11 or MD-80/90 series aircraft.

A key feature of the MD-XX aircraft is the high aspect ratio composite wing which is aerodynamically more efficient than the comparable metal wing (Figure 4). The more efficient and lighter wing will require smaller control surfaces, smaller engines and lighter support structure. The entire aircraft resized will weigh 7300 lb less than its metal wing counterpart. The combined effect of a lighter and more efficient aircraft is to reduce the direct operating cost (DOC) by 2.1 percent, translating into more than 100 percent profit increase for the airlines.

A study was performed to predict production costs of the composite and metal wing aircraft (Figure 5). Learning curves applied to the metal boxes were based on industry history related to the amount of automation used. A less advantageous learning curve, having a constant value of 87 percent, was applied to the S/RFI process because of its highly automated nature. The study proved that the application of composite primary structure to the wing box of the MD-XX will result in a cost-effective solution.

Semi-Span Wing Design

The baseline wing configuration is given in Figure 6. The wing is a two spar, multiple rib structure. The skin is reinforced with blade stiffeners. The 41-foot wing segment, denoted the semi-span wing, was selected to be designed and tested under the current program. This length

was determined as being the maximum that could be comfortably accomodated within a conveniently available company autoclave.

The components of the structural test box shown in Figure 7 consist of upper and lower cover panels, front and rear spars, ribs, bulkheads, and attach fittings for the main landing gear and the engine pylon. The cover panels are the major components and account for approximately 75 percent of the total box weight. The skins, stringers, the intercostal clips and the spar webs are made with S/RFI manufacturing process. The rest of the components are made from conventional prepreg tape material.

The skin preforms are manufactured in the form of discrete stacks each containing nine unidirectional layers (Figure 8). The upper skin stacks utilize the low-cost Hercules AS4 fiber system. Since higher open hole tension allowables are required in the lower cover in order to increase the gross stress level, the decision was made to substitute higher-strength IM7 fibers for AS4 in the 0^0 direction.

The wing skins, being part of the aerodynamic profile, have contoured double curvature surfaces (Figure 9). These curvatures are more severe on the lower skin where the stringers have to be made in the form of curved triaxially woven braided socks stitched together. The other benefit of braiding is that it is a more automated, and therefore more cost effective manufacturing process. Double curvature of the lower skin presented another problem from a design point of view. Since the individual stack pieces would not follow the surface without wrinkling, the skin will be made in two individual stitched parts which will be spliced longitudinally prior to curing.

Design Requirements and Allowables

The effort to design an all-composite wing is based on the "building block" approach to engineering. Under this approach, the wing structure is subdivided into a number of simple subcomponent structures which are then designed, analyzed and tested. This allows us to fine-tune and validate the analysis techniques, to record valuable lessons learned during the process and, as the sufficient experience is gathered, to move on to larger, more complex structures. In many instances, the purpose of the subcomponent tests is simply to derive an allowable stress or load. Numerous subcomponents have been tested to date, Ref. 8, some of which are shown in Figure 10.

One of the central tasks in designing a new structure such as the S/RFI wing is to formulate the appropriate design and failure criteria which would guarantee the structural integrity of the component, and at the same time not incur an unnecessary weight penalty. The following design criteria (Figure 11) have been selected on the basis of past design experiences, Federal Aviation Regulations (FAR-25) and the FAA Advisory Circulars, Ref. 4-5.

- Discrete Source Damage. This type of damage occurs in flight or on the ground and is a result of collision with a foreign object such as another aircraft, building, bird or vehicle.

Severe in-flight damage might be encountered after a major engine disintegration. For the purposes of this program, the extent of the discrete source damage is to include a completely severed stringer and the skin on either side up to the flanges of the adjacent stringers. Since the aircraft exposed to such damage will be immediately repaired, it is extremely unlikely that peak loads of the flight envelope would be encountered in the time interval between the described event and landing. A structure with discrete source damage must therefore be able to withstand only 70 percent of the design limit load (DLL) without catastrophic failure and only flight conditions must be considered.

- Detectable (visible) Damage. When a structure is damaged to a lesser extent than during the discrete source damage event, the damage may remain undetected during the regular inspection intervals. During such time the structure is required to carry 100 percent of DLL. To be detectable, the indentation due to damage must be at least 0.1 inches in depth. Once the damage is detected, the damage site is repaired.

- Non-Detectable Damage. When the impact event produces no visible symptoms or a dent depth of less than 0.1 inches, damage is considered to be non-detectable, and the structure must be able to survive full design ultimate load (DUL). The impact energy up to 100 ft-lb for the exterior surfaces and up to 20 ft-lb for the interior surfaces must considered in the stress analysis of every structural component. It is conceivable that the 100 ft-lb impact, sometimes even a lower energy impact, may produce a detectable dent in thin laminates. In such cases, the impact energy level must be reduced until the level which produces a 0.1" dent is found.(Recall that dents deeper than 0.1" are classified as detectable). Conversely, a 100 ft-lb impact rarely produces detectable damage in thick laminates, while higher impact energies being unlikely events should not be considered.

- Reparability If a structure is exposed to damage of such an extent that the damage can be detected by visual inspection, the affected structural site will be repaired. The structure in the repaired configuration is required to withstand the same set of loads as in the unrepaired state. The repairs must therefore be designed to carry the design ultimate load (DUL).

As part of the subcomponent analysis phase of the program, work was performed to determine all of the required material and structural allowables which would satisfy the applicable design criteria listed above. Whenever possible, testing was preceded by analysis to predict the structural response and to calculate the final failure loads. Based on the comparison of analysis and test, analytical models were either validated, or improved to match the test data. In some cases, as in the case of analysis for the discrete source damage, the analytical models produced results so different from test that they were found to be of limited usefulness. In such cases, the decision was made to derive the allowable stresses on the basis of test alone.

In order to design a wing structure for the effects of the discrete source damage, it was postulated that the result of this type of damage would most likely be a completely severed stringer including the skin on either side. The total length of the through crack was taken to be seven inches. To differentiate between the upper and lower covers, tension and compression cases were examined separately, Figure 12. Shown in this figure also are panels used for

measuring the panel residual strength after a 100 ft-lb impact event. Figure 13 gives the photograph of the test panel instrumented with strain gages in which damage was simulated by a seven inch saw cut through the middle stringer.

The analytical model for the discrete source damage analysis was based on the classical point stress criterion (Ref. 10). A fine grid finite element model was constructed to determine the stress distribution in the vicinity of the crack tip. The calculated initial crack propagation stress closely matched the test data. Although the model was able to predict a stable crack growth as the crack extended towards the adjacent stringer flanges, the calculated final failure stress was off by a factor of 2. The difference was attributed to the fact that the point stress criterion in its original form does not adequately describe the entire range of different crack lengths without the help kind of empirical correction factors. These, for example, can be defined such as to make the characteristic distance a function of the crack size. The other reason for the discrepancy could be the complex nature of the stress state in the configuration where the crack is extended all the way to the flanges of the adjacent stringers. Detailed 3-D FEM analysis utilizing fracture mechanics techniques appears to be the most promising tool for solution of such problems.

It is interesting to note that the discrete source damage tension and compression panels showed a very different structural response during test, Ref. 2. In the tension panel, Figure 14, the crack propagated to the flanges and, as the load increased, changed the direction and extended along the side of the flange. The panel ultimately failed at the grips, never reaching its full structural potential. The crack in the compression panel, on the other hand, never changed its course and grew under the flange of the stringer causing failure of the panel, Figure 15. Both panels demonstrated that stitching helped prevent skin-to-stiffener disbonds which is a typical failure mode of the conventional pre-preg composites.

The gross area stress ultimate design allowables derived from test were 50.8 ksi and 80.6 ksi for the upper and lower covers respectively. The tested tension panel was made up of AS4 fiber. The wing lower cover is made from the higher strength IM7/AS4 hybrid material which makes it possible that even higher residual strength may be attained. Overall, such high values of the gross stress allowables make the discrete source damage design criterion less critical relative to other structural criteria such as reparability and tolerance to non-detectable damage.

The tests have confirmed the theory that stringers play a major role in arresting one- or two-bay cracks resulting from a discrete source impact. The crack arrestment capability of a panel can best be described in terms of a stiffening ratio, the ratio of stiffness of a stringer to that of a bay. The stiffening ratio of the tested panel was 35%. All the cover panels of the semi-span wing are being sized to this stiffening ratio. Since the exact mechanisms of the crack arrestment phenomenon are still not completely understood, an additional design requirement is imposed on the wing stringer geometry. The ratio of the flange thickness to the combined thickness of skin and flange is being kept at approximately 40% to match that of the tested panel.

As was mentioned earlier, tests have shown that the wing reparability requirements are by far the most important criteria governing the selection of the maximum working stress level in the covers of the semi-span wing. Operational requirements dictate the need for a capability for

installing rapid and inexpensive repairs in the wing covers under austere field conditions. There is also an additional requirement that the repairs can be accomplished with conventional non-perishable materials. A design solution utilizing bolted-on metal patches was rated as the most promising repair concept for the semi-span wing, Ref. 2.

Two different repair scenarios were formulated. The first scenario addresses the repair of wing skin with detectable or discrete source damage sufficiently localized so that the stringers adjacent to the damage site remain unaffected. To avoid a potential long term material degradation and to prevent possible fuel leaks, the material around the damaged area must be removed. The shape of the clean-up area was determined from a finite element analysis optimization study. An elliptical hole with the major axis aligned with the longitudinal direction and with its minor axis spanning the distance between the adjacent stringers was selected as causing the minimum local stress concentrations. Although the structure in the clean-out configuration retained a sufficient amount of ultimate strength, the installation of a mechanically fastened doubler was nevertheless necessary in order to meet the aerodynamic and the fuel containment requirements of the wing. The repair was demonstrated on a four stringer panel with an elliptical cut-out (1:2 eccentricity ratio) covered by a .125-in. 7075-T6 aluminum doubler fastened with .375 in. titanium bolts.

The second repair scenario involves repairs of a damaged or completely severed stringer. As before, the affected site is cleaned out by introducing an elliptical cutout. The removed part of the damaged stringer is replaced by an aluminum substitute, and the entire area is covered with a metal doubler attached to the skin by means of mechanical fasteners. The repairs of this type were investigated on a five-stringer panel. A typical wing cover location for such panel is shown in Figure 16.

The tests of the five-stringer and the four-stringer (Figure 17) repair panels verified the required ultimate capacity of the repaired structures in terms of the allowable gross stress level. The upper cover is currently being designed to withstand 40 ksi of gross ultimate compression stress. The lower cover, being composed of a superior strength hybrid material with IM7 fiber, is designed to 50 ksi gross ultimate tension stress. Although the above stress allowables are assumed to apply universally to any location within the wing, further work may be required to investigate whether any fine-tuning or modifications in the proposed repair concept are required for some local regions in the wing such as spar caps and access doors, or for any other locations where loading or the geometry are drastically different from the tested configurations. Some of this work is being planned for the later phases of the wing development project.

The current status of stress allowables corresponding to various structural design criteria and compared to the required structural capacity is given in Figure 18. The figure demonstrates that all the structural design goals set for the development of the semi-span wing are being met successfully.

The gross allowable stress of 40 ksi and 50 ksi for the upper and lower covers respectively in general satisfy only the reparability requirement of the wing. It has been observed that the undetectable damage criterion is more restrictive than the reparability condition when moderately thin laminates are considered. Predicting the residual strength of a composite structure subjected

462

to impact is a complex task which is still a topic for much of the ongoing research within the stress community. Many of the proposed solutions requiring an intensive computational effort, such as a progressive failure model, are clearly unacceptable for a production type of design effort. In response to the need for a simple, yet effective theory, NASA has developed a parametric damage model, Ref. 6.

The parametric damage model assumes that the residual strength of a structure depends on a single damage parameter. It has been found that the damage parameter giving the best fit to the experimental data is a maximum impact force divided by the square of the laminate thickness, Figure 19. The impact force is calculated from an energy balance equation and should include the stiffness and inertial characteristics of the impacted structure. The parametric damage model makes it possible to apply the information gathered from coupon testing for prediction of the compression-after-impact strength (CAI) of an actual structure by relating both to the same parameter.

It is important to note that for the same level of impact energy and the same thickness, the residual strength of a structure will typically be higher than that of a coupon, because coupons, being stiffer, usually develop higher impact forces. This observation allows us to conservatively utilize the CAI strength obtained from coupons and apply the methods of the parametric damage model only to those locations in the wing which operate at low safety margins. This simplifies the design process by allowing the construction of a single stress allowable curve applicable to a wide range of laminate thicknesses, Figure 20. A similar curve is currently being prepared for the lower cover laminates except that, besides the CAI strength, it also addresses the tension-after impact allowable strength (TAI).

In addition to the structural design criteria whose function is essentially to prescribe the allowable stress level within the wing, there are a number of manufacturing requirements which have to be addressed in the design process. The maximum depth of the stringer plus skin is set at 4.0 in to satisfy the stitching machine constraint shown in Figure 21. The maximum number of skin stacks which can be stitched by a multi-needle machine is currently nineteen (each stack is .054 in. thick). In order to be able to utilize a multi-needle machine for stitching of the upper cover blades, the blade thickness must be limited to a maximum of ten stacks. Skin stack drop-offs must accomplished one at a time to minimize the joggle of the stringer blade, Figure 22.

The design of a real wing structure which eventually will be flown on an actual airplane is a complex and involved process which requires a careful consideration of all the various design issues. Many of these issues, which have been omitted in this paper due to its limited scope, can be found in Ref. 1. Among these are the tooling development, design for lightning protection, fuel and other systems issues.

Analysis Methodology

Reliable analysis methods are required in order to minimize the risk associated with the development of a new all-composite wing. The analysis methodologies developed during the

463

preliminary phases of the project and used for the analysis of the semi-span wing will be ultimately validated when the wing box is tested at NASA Langley. Many of the techniques have already been validated during the subcomponent tests phase of the project. Among these are the modified lamination theory, composite joint analysis techniques, the parametric damage model.

The development of the modified lamination theory was necessitated by the fact that the ultimate strength and stiffness of a stitched warp-knit material are affected by crimping of the load carrying fibers. The problem was solved by assuming that the extent and the effect of the crimping was a function of the fiber orientation. The material properties of each layer within a stack were assigned based on the layer's direction relative to the stitching path. Table 1 lists the laminae properties which were derived from test.

Table 1. Stitched Lamina Material Properties

Lamina Properties	0-degree	45-degree	90-degree
E_l (msi)	18.0	17.7	17.5
E_t (msi)	1.62	1.62	1.62
G_{lt} (msi)	.80	.80	.80
ν	.34	.34	.34
F_{lt} (ksi)	225.	200.	185.
F_{lc} (ksi)	145.	140.	135.
F_{tt} (ksi)	5.	5.	5.
F_{tc} (ksi)	31.	31.	31.
F_{sh} (ksi)	17.5	17.5	17.5

The unnotched strength properties of a laminate are rarely used in the strength analysis of a composite component, because it is the notched allowables and the CAI strength which are the critical parameters governing the load carrying capability of the component. The unnotched laminate properties are nevertheless important for defining the reference strength in the off-axis directions. This off-axis strength is used for establishing the open- and loaded-hole strength of the wing laminates. The method for calculating these is based on the stress concentration theory of J. Hart-Smith, Ref. 9.

The theory, originally developed for uniaxially loaded composite holes and recently generalized to include the effect of biaxial loading, is based on a postulate that the degree of stress relaxation at the surface of a hole is linear with the stress concentration factor acting on the net section. The theory is functionally equivalent to the point stress method (Ref.10), and in fact reduces to it in the case of an infinitely wide plate. Unlike the point stress method, Hart-Smith theory cannot account for the hole size effect and for the effect of the off-axis loading. An extensive testing program was therefore undertaken to fully characterize the wing cover laminates by considering

all the various hole sizes and load orientations. The results of the test were cast in terms of the stress reduction coefficients referred to as the C-factors.

Although the C-factor approach does require more coupon testing than the point stress method, the method has some definite advantages over the point stress method, especially in situations when the bearing-bypass interaction type of analysis is required. It has been observed that the loaded hole analysis based on the characteristic distance derived from tests of the open hole coupons does not correlate well with the test results. Since in the C-factor theory the stress reduction coefficients are defined for the separate loaded - and open-hole problems, a better match to the experimental data can be obtained. This improved accuracy was especially important when the repairs of the wing cover, the root splice area and the Main Landing gear attachment were analyzed. The analysis of the latter presented a particular challenge since the directions of the by-pass and bearing loads, as well as the material direction of the skin laminate were all misalligned relative to each other.

The methodology of analysis for damage tolerance is based on the parametric damage model described earlier. In the course of the stress analysis of the lower cover access holes, a limitation in the application of the parametric damage model method was encountered. High stress concentrations on the surface of an access hole make it very conservative to directly utilize the TAI allowable stress which is by definition a measure of the far field failure stress. Improvements to the method are being studied.

To determine the internal load distributions in the wing, a FEM model of the semi-span wing , Figure 23, has been constructed in PATRAN 3.0 and executed in NASTRAN This model serves as the global element in the global-local analysis process. Some of the local fine-grid FEM models representing the critical subcomponents are shown in Figure 24. The global FEM model of the wing will be used to perform global buckling analysis, once sizing of all the wing components is completed. According to the design criteria, neither the global nor local buckling modes are permitted to occur in any structural component of the semi-span wing. Since the stringers are designed to have stable cross-sections, they are analyzed as continuous multi-span beam-columns deflected laterally to match the wing deflected configuration. Failure of a stringer is assumed to occur when the combined axial and bending stress at the edge of a blade exceeds the CAI allowable stress.

Conclusions

The development effort to design and build an all-composite wing structure has been presented. It is demonstrated in this paper that all the cost and weight targets which make the all-composite wing an attractive alternative to a conventional metal wing are being met. The success of the program is largely due to the outstanding damage tolerance characteristics and low cost associated with the S/RFI process. Up to this point in the wing development program, no major problems have been encountered in design, analysis or manufacturing. The program successfully passed the preliminary design review (PDR) with NASA in March 1994, and a full development

effort is underway now to prepare for the critical design review (CDR) to be held in August 1995.

Acknowledgments

References

1. Hawley, A. V.: Preliminary Design of a Transport Aircraft Composite Wing, Fifth NASA/DoD Advanced Composites Technology Conference, Aug. 1994

2. Sutton, J.O, Jegley, D., Kropp, Y., and Banister-Hendsbee, D. L.: Design, Analysis, and Test of Composite Primary Wing Structure Repairs, Fifth NASA/DoD Advanced Composites Technology Conference, Aug. 1994

3. Hawley, A. V. and Sutton, J. O.: Design and Analysis Consideration for Stitched/RTM Composite Wing Structure, NASA CP 3229, 1993

4. Department of Transportation, FAA, Federal Aviation Regulations Part 25 - Airworthiness Standards: Transport Category Airplanes

5. "Damage Tolerance and Fatigue Evaluation of Structure", FAR Advisory Circular, AC 25.571-1a, March 5, 1986

6. Jackson, W. C., and Poe, Jr. C. C.: The Use of Impact Force as a Scale Parameter for the Impact Response of Composite Laminates, NASA TM 104189, January 1992.

7. Hinrichs, S. , Chen, V., Jegley, D, Dickenson, L.C., Kedward, K.: Effect of Impact on Stitched/RFI Compression Panels, Fifth NASA/DoD Advanced Composites Technology Conference, Aug. 1994

8. Burwasser, J. T., and Stewart, T. Z.: Composite Wing Verification Subcomponents, Fifth NASA/DoD Advanced Composites Technology Conference, Aug. 1994

9. Nelson, W. D., Bunin, B. L., and Hart-Smith, L. J.: Critical Joints in Large Composite Aircraft Structure, NASA CR-158902-2, July 1978

10 Deaton, J. W., Dexter, H. B., Markus, A. M., and Rohwer, K. M.: Evaluation of Braided Stiffener Concepts for Transport Aircraft Wing Structures, Fifth NASA/DoD Advanced Composites Technology Conference, Aug. 1994

10. Whitney, J. M. and Nuismer, R. J. : Stress Fracture Criteria for Laminated Composites Containing Stress Concentrations, J. of Composite Materials, Volume 8, July 1974

Fabric Manufacture

Automated Creation of 9-Ply Stack
(0, ±45, 90) Continuous Material

Stitched Preform

Automated Stitching of Multi 9-Ply
Stacks, Rib, and Spar Cap Webs

RFI Process

Simple Autoclave Process
Without RTM Complications
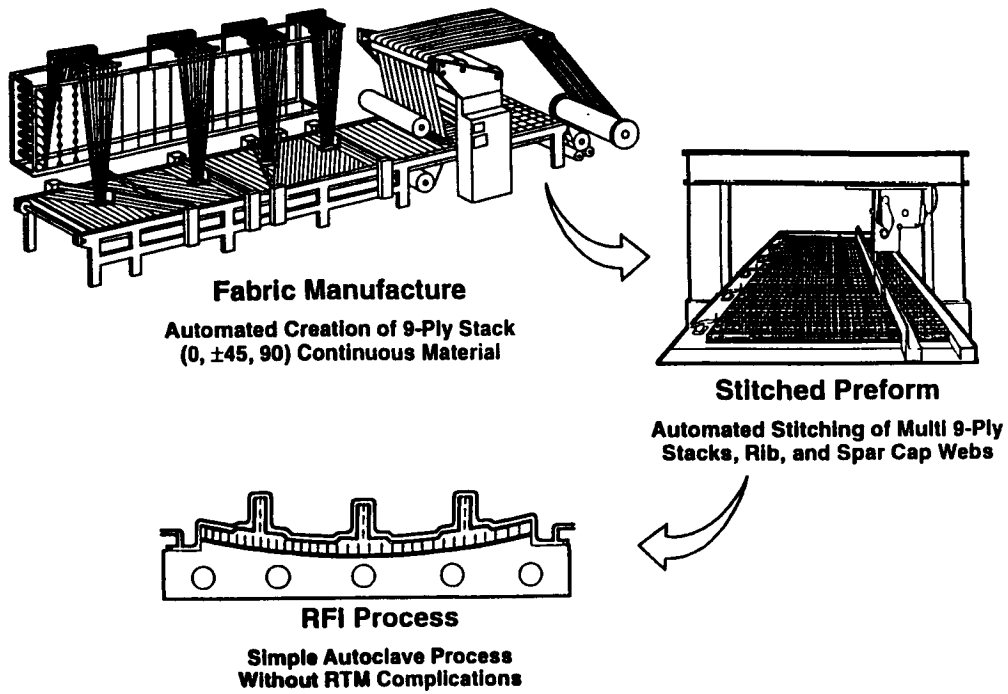
Figure 1. Stitched RFI Manufacturing Process

MD-XX Transport Aircraft
D-3308-4 configuration
192 passengers
Wing span = 129 ft. 4.5 in.
Wing area = 1385 sq. ft.
Wing aspect ratio = 12.1
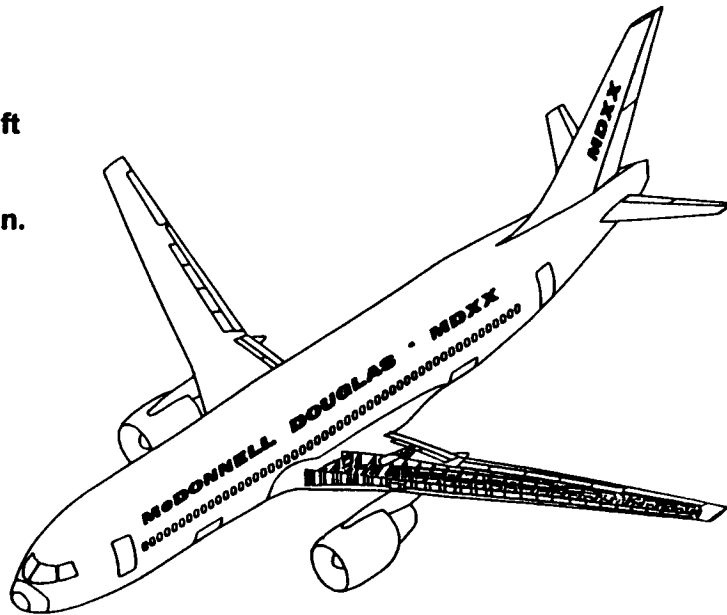
Figure 2. Baseline Aircraft

Radome
Tailcone
Fairings
Nacelles
Fuselage Floor
Stabilizers
Control Surfaces
L/G Doors
Wing Box

Figure 3. MD-XX Composite Applications
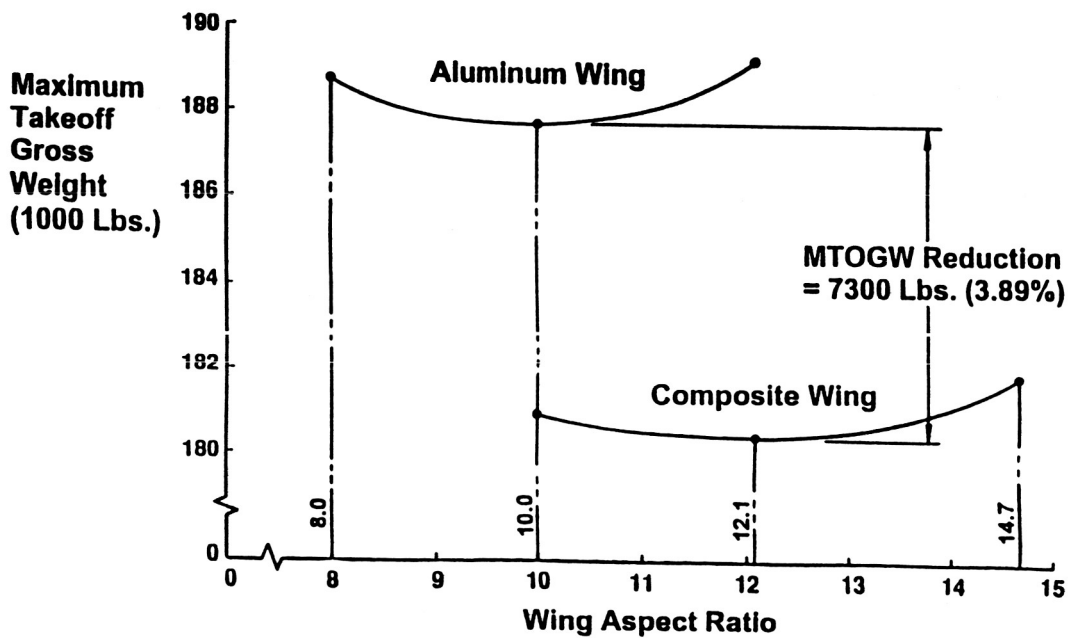
Figure 4. Aircraft Aspect Ratio Study

600 Unit Production
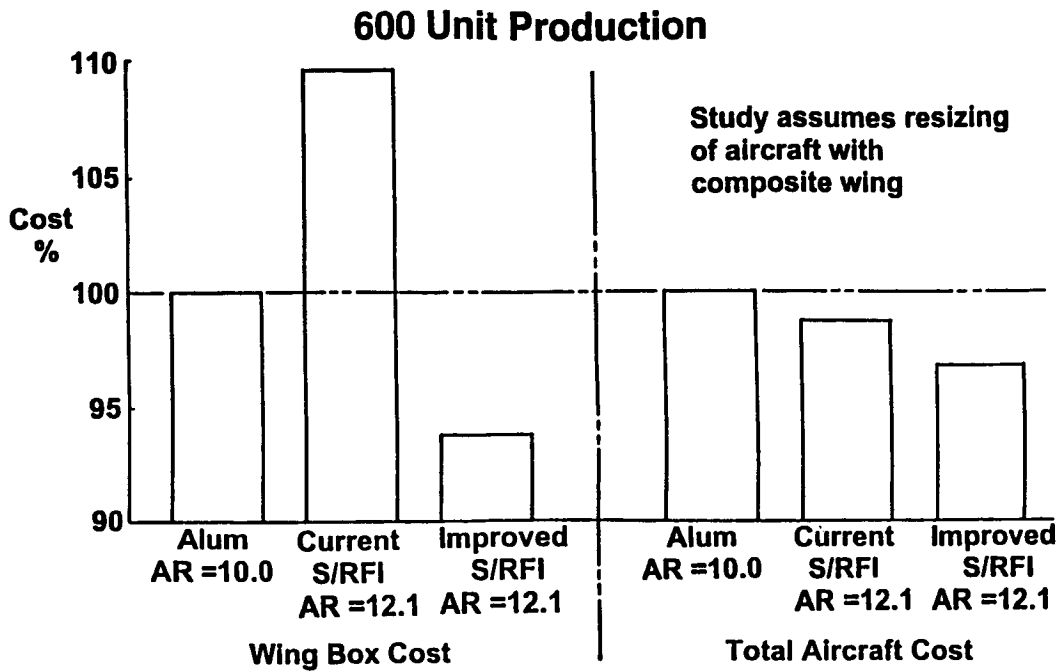
Figure 5. Aircraft Cost Study

□ **2-spar configuration**
□ **Ribs perpendicular to rear spar**
□ **Test box length limited by available autoclave**
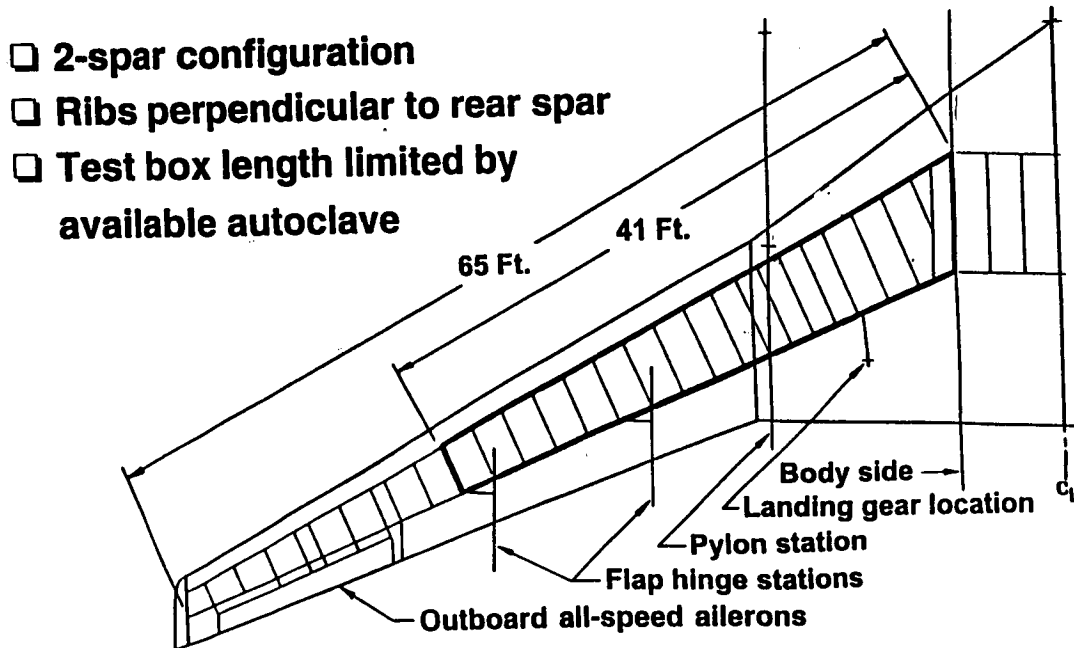
Figure 6. Baseline Wing Configuration
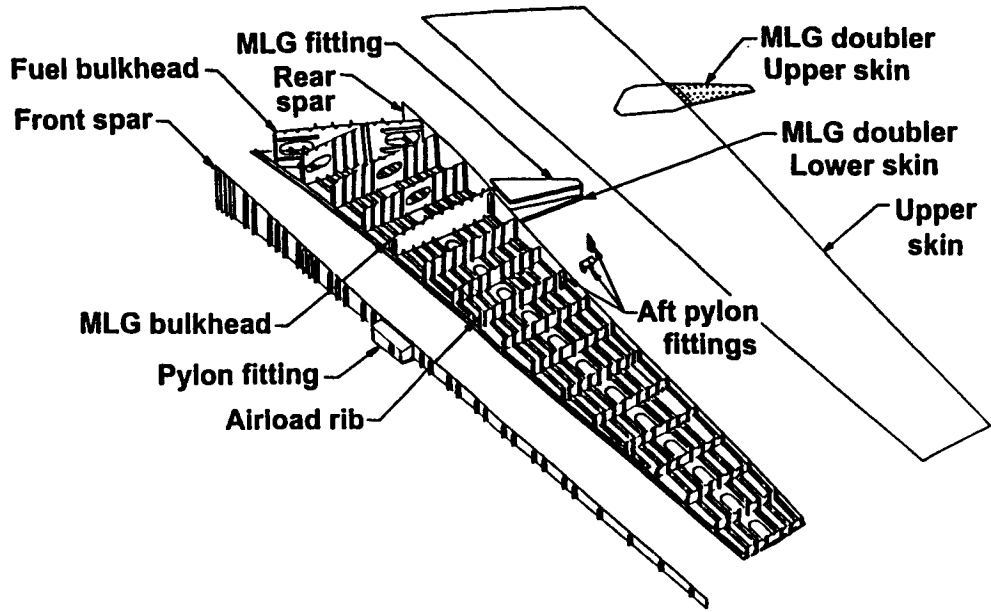
Figure 7. Structural Wing Box Components

LAYER DIRECTION	AREAL WEIGHT (g/m²)	FIBER MATERIAL	
		TYPE 1 (UPPER)	TYPE 2 (LOWER)
45	153	AS4	AS4
-45	153	AS4	AS4
0 0	320	AS4	IM7
90	173	AS4	AS4
0 0	320	AS4	IM7
-45	153	AS4	AS4
45	153	AS4	AS4
TOTAL	1425		

Fiber percentages

0 : 44.9
45 : 42.9
90 : 12.2

0°

Stringers and spar caps
Upper : Type 1 stacks
Lower : Braided construction
using similar layup

Stack width = 120 in. minimum
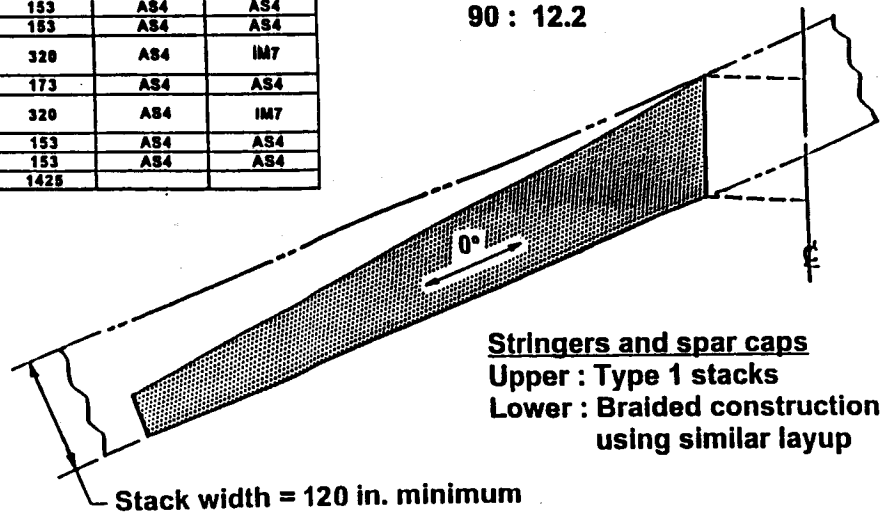
Figure 8. Preplied Laminate Stack

View along length of cover panel
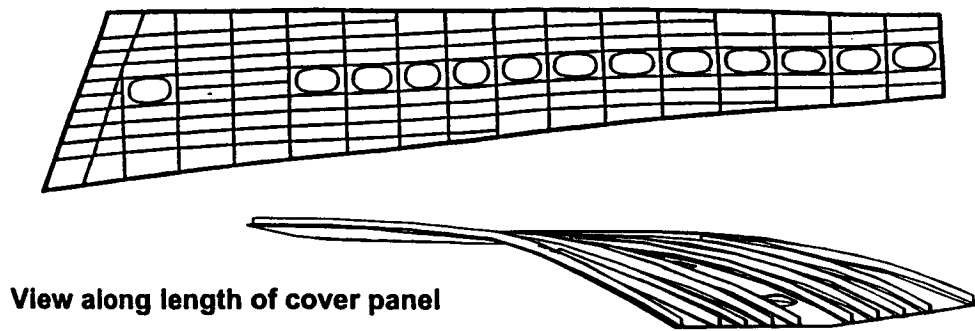
- ❑ Twisted double curvature surface
- ❑ Fuel access holes midway between spars
- ❑ Stringer planes determined by door locations

Figure 9. Wing Lower Cover

Spar Cap Tension

Stringer Pull-Off

Spar Cap Shear

Rib Clip Tension

Stringer Runout Configuration, Intermediate Box.
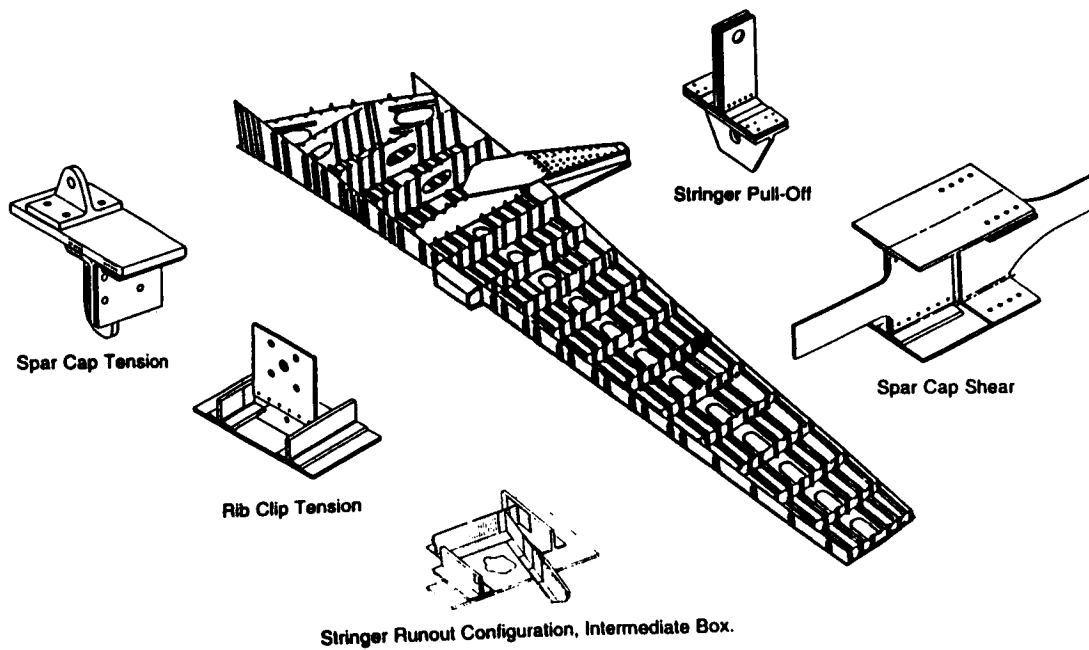
Figure 10. Subcomponent Test Program
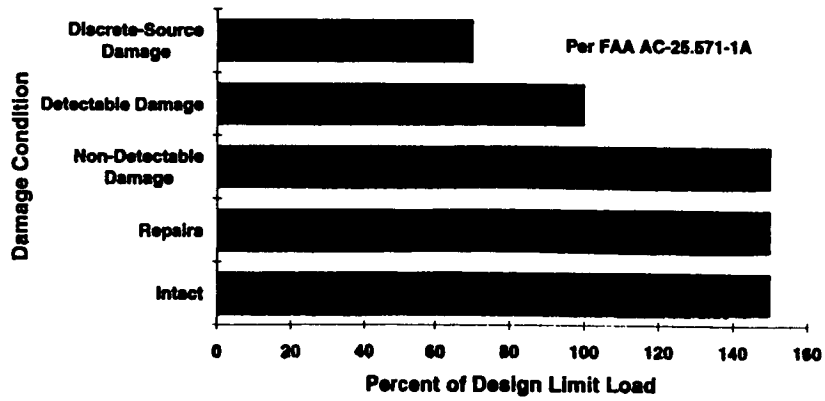
Figure 11. Composite Wing Design Criteria

COMPRESSION   TENSION

Detectable Damage   Discrete-Source Damage   Discrete-Source Damage   Detectable Damage
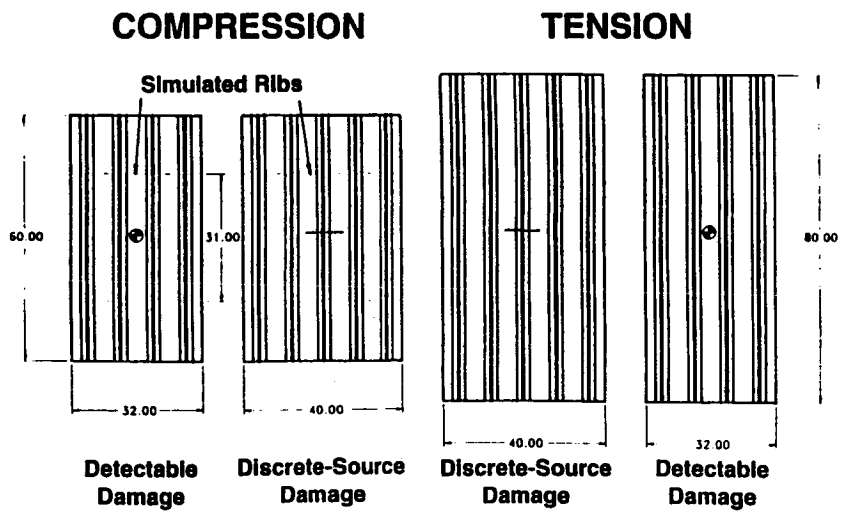
Figure 12. Wing Cover Damage Tolerance Test Panels
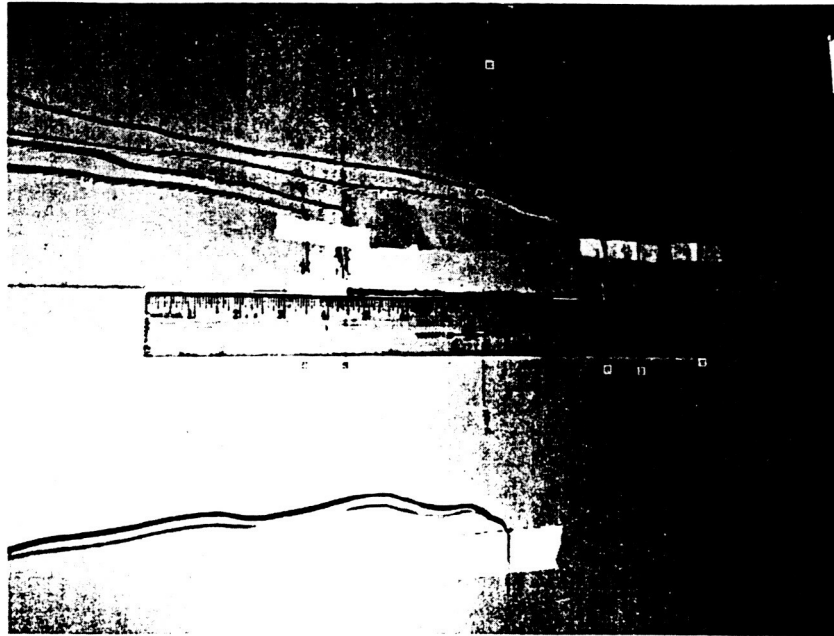
Figure 13. Panel with Discrete Source Damage
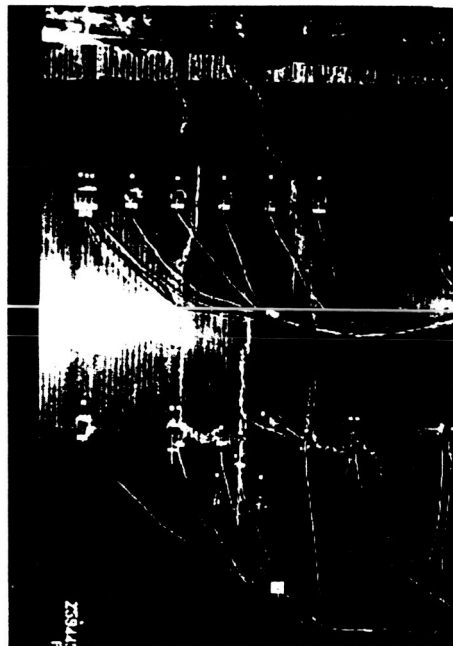
Figure 14. Failure of Discrete Source Damage Tension Panel

Figure 15. Failure of Discrete Source Damage Compression Panel
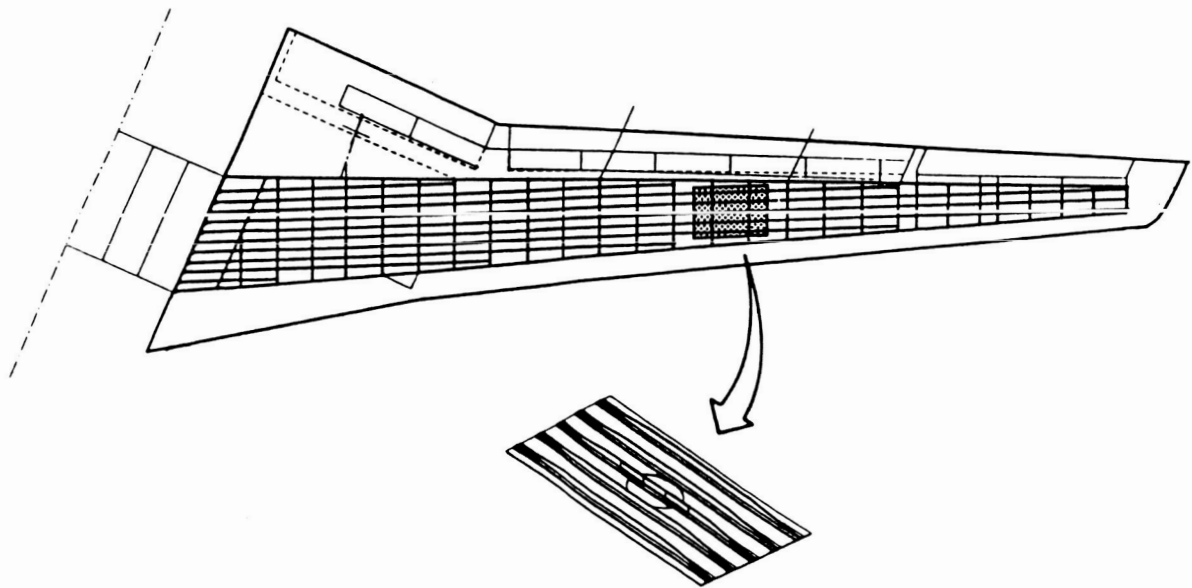
Figure 16. Location of Test Repair Panel

Figure 17. Failure of Repaired Compression Panel
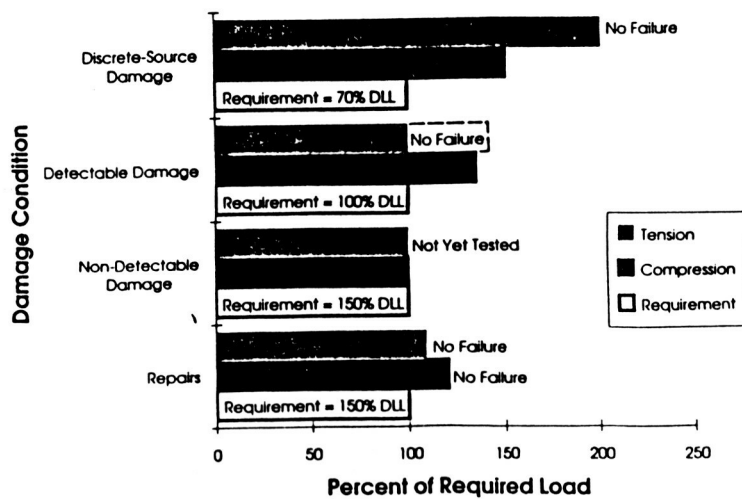
Figure 18. Design Criteria vrs Test for the Semi-Span Wing
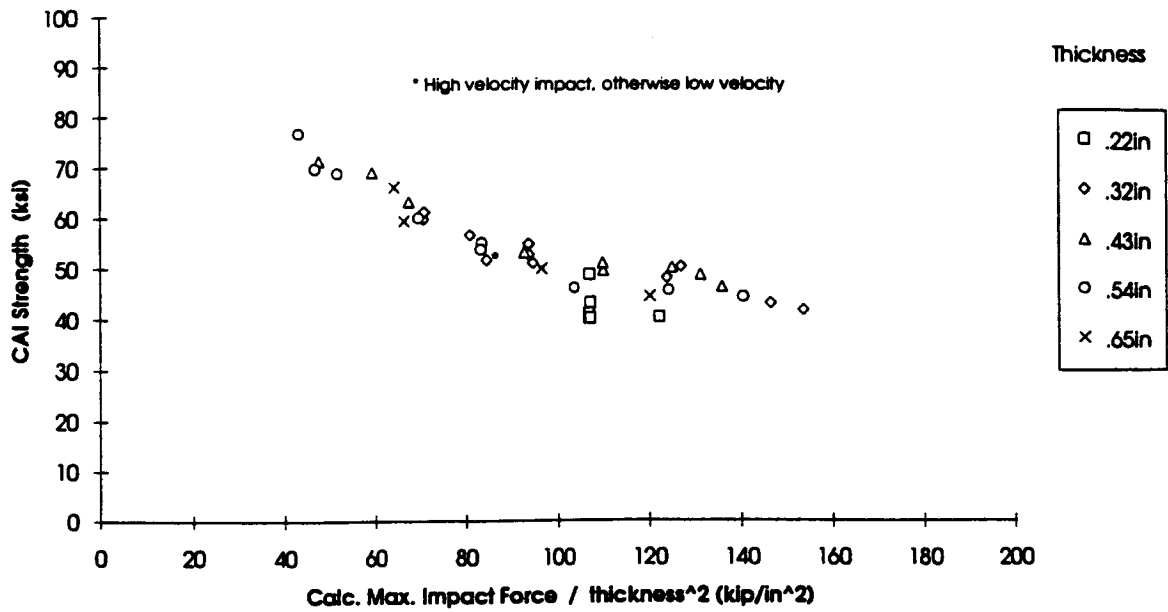
Figure 19. CAI Strength For Wing Upper Cover
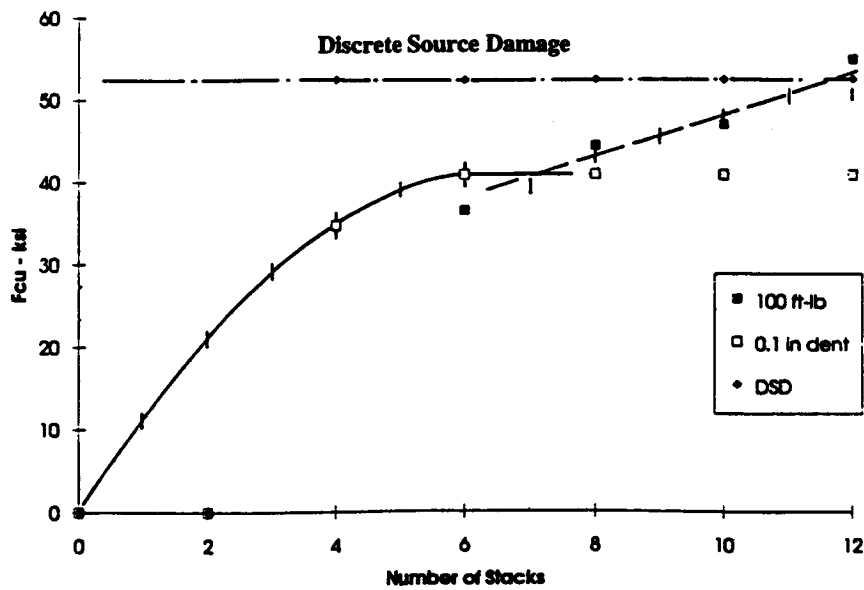
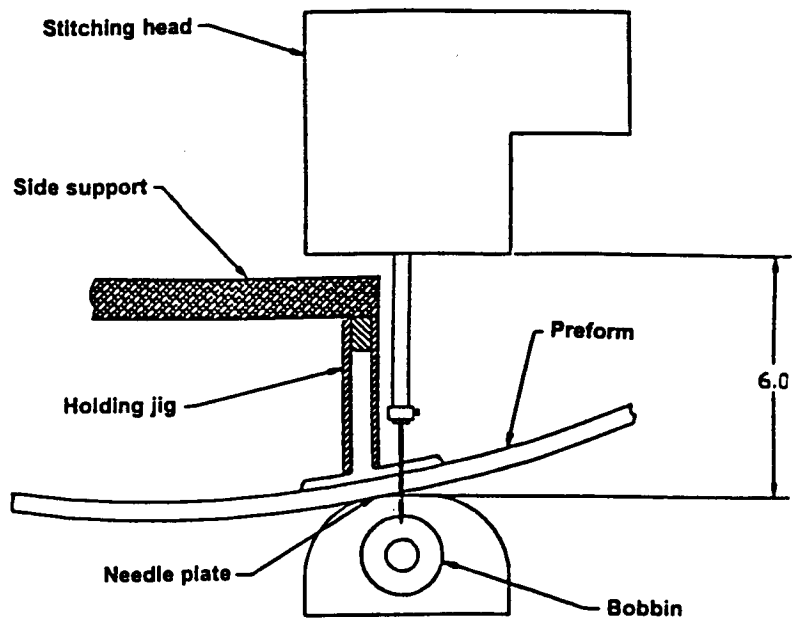**Figure 20. Upper Cover Allowable Stress for Damage Tolerant Design**
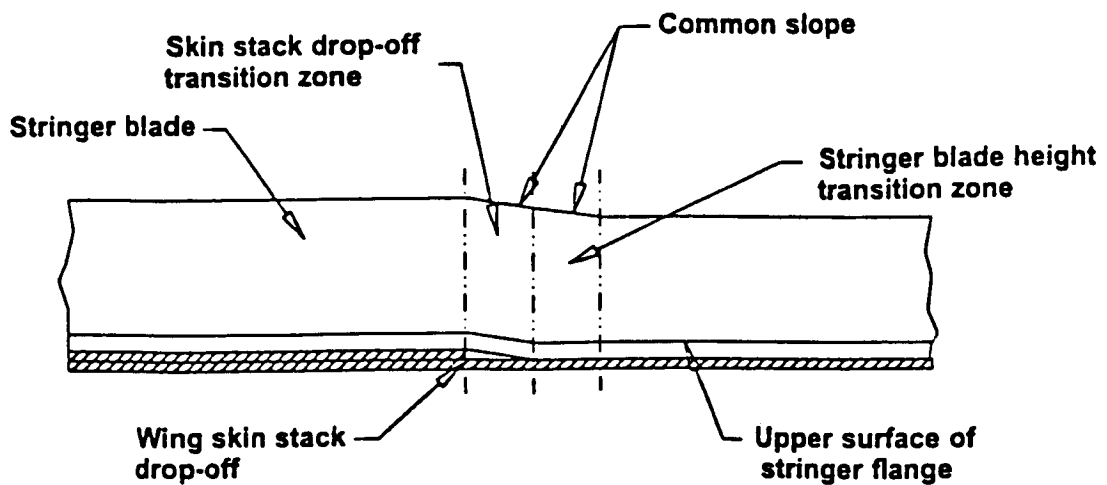
Figure 21 Stitching Head Clearance Constraint

Figure 22 Stringer Height Transitions
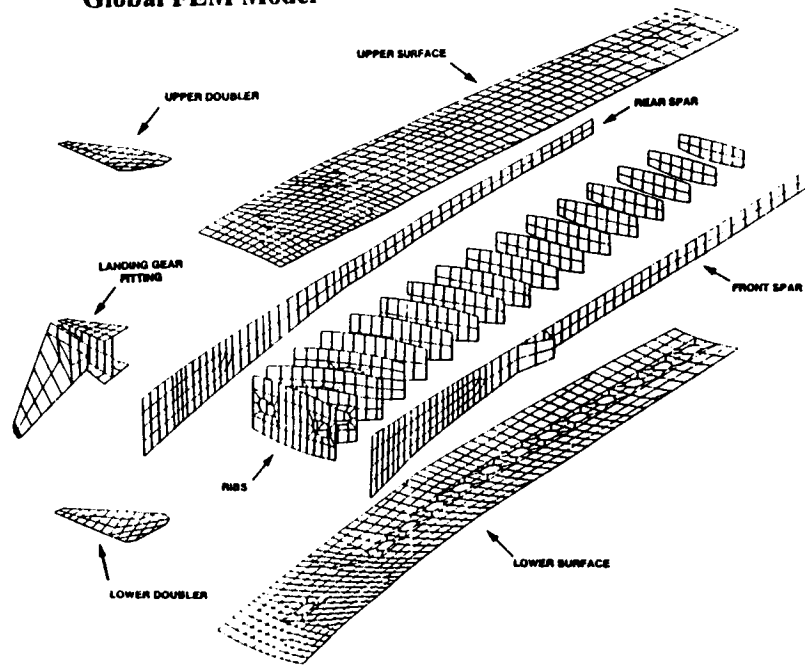
Global FEM Model
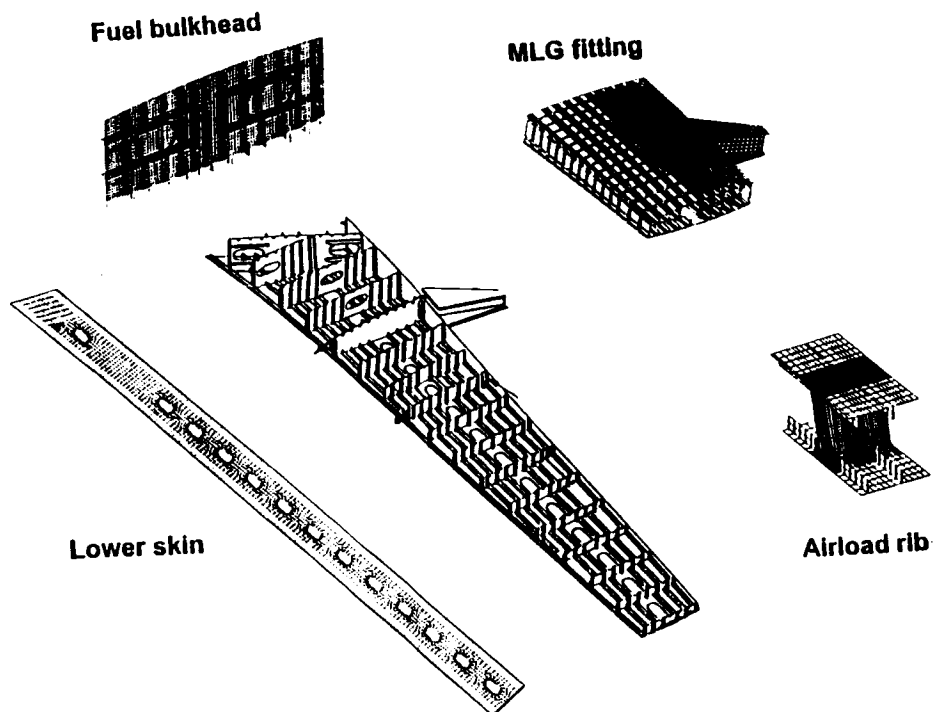

Figure 23 Global FEM Model of the Semi-Span Wing

Figure 24 Global/Local Analysis of Critical Components.